Unified treatment of atomic excitation and ionization

N. W. Antonio,[1,*] I. Bray,[1,†] and A. S. Kadyrov[1,2,‡]
[1]*Department of Physics and Astronomy, Curtin University, GPO Box U1987, Perth, WA 6845, Australia*
[2]*Institute of Nuclear Physics, Ulugbek, 100214 Tashkent, Uzbekistan*

(Received 27 May 2024; accepted 28 August 2024; published 12 September 2024)

A unified treatment of atomic excitation and ionization in ion-atom collisions is proposed. It is demonstrated that the state-resolved excitation cross sections multiplied by n^3, where n is the principal quantum number of the excited state, and the corresponding partial singly differential ionization cross section form two parts of a single continuous function. This allows one to obtain the excitation cross section for any state including high-lying Rydberg states and the energy-differential ionization cross section at, and arbitrarily close to, the threshold. The proposed method can be used in any theoretical approaches to excitation and ionization and experimental measurements.

DOI: 10.1103/PhysRevA.110.032810

I. INTRODUCTION

The physics of quantum collisions is fundamental to our understanding of the universe at its most basic level. It has practical applications in many areas of science and technology, including clean energy production, medicine, and astrophysics. When a projectile collides with an atomic or molecular target it may scatter elastically or lead to excitation of the target. It can also ionize the target and induce various other processes depending on the nature of the target and the projectile. An interesting aspect of the ionization process in atomic collisions is its relationship to excitation. This feature has been of interest since the early days of quantum mechanics. In fact, as early as 1924, Sommerfeld [1] predicted that the oscillator strengths from the discrete states merge with the differential one from the continuum at the ionization threshold. This theory is now a cornerstone in the field of photon-atom scattering [2,3]. Furthermore, based on the Oppenheimer scaling rule [4], Rudd and Macek [5] suggested that the average excitation cross section below the ionization limit merges continuously with the ionization cross section above the ionization limit in ion-atom collisions. They concluded that the transition across the threshold is a slowly varying function of energy loss by the projectile (see Fig. 45 of Ref. [5]).[1] The idea has not been further developed.

In this paper, we quantitatively show a continuity between excitation and ionization. We introduce a continuous function that unifies these scattering processes. It links the state-selective excitation cross sections and the corresponding partial singly differential ionization cross section. We then demonstrate how this function can be used to give the state-resolved target-excitation cross sections for any bound state including Rydberg ones. Furthermore, it gives the energy-differential ionization cross section at, and arbitrarily close to, the ionization threshold.

II. THEORY

We consider scattering of an incident ion on an arbitrary atomic target. The target can initially be in its ground state or any excited state including a Rydberg one. We assume that the collision energy is sufficient to ionize the target, i.e., the total energy of the collision system $E_{\text{total}} > 0$. Following the collision, the atomic electron may be excited to a discrete eigenstate with energy[2] $E_n = -1/(2n^2)$, where $n = 1, 2, \ldots, \infty$ is the principal quantum number. Alternatively, the electron may be excited into the atomic continuum with energy $0 \leqslant E \leqslant E_{\text{total}}$. Let us generalize n into a continuous variable x. This makes energy also a continuous function of x, E_x. Then only integer values of x have a physical meaning of the principal quantum number and only corresponding values of E_x have a physical meaning of the bound-state energy.

From a physical point of view we assume there is little difference between excitation of the high-lying Rydberg states and near-threshold ionization. Therefore, we introduce a continuous function of electron energy, $S(E)$, that is common for both excitation and ionization. Function $S(E)$ is not completely unknown. Its first-order derivative in E for $E > 0$ is a measurable quantity known as the singly differential ionization cross section (SDCS), $\mathrm{d}S/\mathrm{d}E$. At the ionization threshold $S(E)$ should behave such that

$$\lim_{x\to\infty} \frac{\mathrm{d}S}{\mathrm{d}E_x} = \lim_{E\to 0} \frac{\mathrm{d}S}{\mathrm{d}E}. \tag{1}$$

The left-hand side can be written as $\mathrm{d}S/\mathrm{d}E_x = (\mathrm{d}S/\mathrm{d}x)(\mathrm{d}x/\mathrm{d}E_x)$. When $x \to \infty$, the continuous energy is given as $E_x = -1/(2x^2)$. Therefore, we have $\mathrm{d}E_x/\mathrm{d}x = 1/x^3$.

*Contact author: nicholas.antonio@postgrad.curtin.edu.au
†Contact author: igor.bray@curtin.edu.au
‡Contact author: a.kadyrov@curtin.edu.au

[1]As it will be seen later, this is not always the case.

[2]Atomic units (a.u.) are used unless otherwise specified. In addition, the target atom is assumed to be neutral; a generalization of the results to partially stripped ions is straightforward.

 ©2024 American Physical Society

Accordingly, Eq. (1) reduces to

$$\lim_{x\to\infty} x^3 \frac{\mathrm{d}S}{\mathrm{d}x} = \lim_{E\to 0} \frac{\mathrm{d}S}{\mathrm{d}E}. \tag{2}$$

We now introduce the following piecewise function:

$$f(E) = \begin{cases} x^3 \mathrm{d}S/\mathrm{d}x & \text{if } E < 0, \\ \mathrm{d}S/\mathrm{d}E & \text{otherwise.} \end{cases} \tag{3}$$

Both pieces of this function have a dimensionality of [area]/[energy]. According to Eq. (2), the function behaves smoothly at the ionization threshold.

We now claim that

$$\left.\frac{\mathrm{d}S(E)}{\mathrm{d}x}\right|_{x=n} = \sigma_n, \tag{4}$$

where σ_n is the cross section for excitation of the n shell. In other words, when x is an integer, the aforementioned derivative has a clear physical meaning and represents the scattering cross section.

In practical calculations, the total SDCS, $\mathrm{d}S/\mathrm{d}E$, comes as a sum of partial SDCS, $\mathrm{d}S_{\ell m}/\mathrm{d}E$, where ℓ and m are the orbital angular momentum and magnetic quantum numbers of the ionized electron. We now extend $S_{\ell m}(E)$ to negative energies. Then a relationship similar to Eq. (2) can be obtained for $S_{\ell m}(E)$,

$$\lim_{x\to\infty} x^3 \frac{\mathrm{d}S_{\ell m}}{\mathrm{d}x} = \lim_{E\to 0} \frac{\mathrm{d}S_{\ell m}}{\mathrm{d}E}, \tag{5}$$

and a corresponding piecewise function be introduced,

$$f_{\ell m}(E) = \begin{cases} x^3 \mathrm{d}S_{\ell m}/\mathrm{d}x & \text{if } E < 0, \\ \mathrm{d}S_{\ell m}/\mathrm{d}E & \text{otherwise.} \end{cases} \tag{6}$$

For completeness, we also introduce $S_\ell(E)$ by summing $S_{\ell m}(E)$ over m:

$$\lim_{x\to\infty} x^3 \frac{\mathrm{d}S_\ell}{\mathrm{d}x} = \lim_{E\to 0} \frac{\mathrm{d}S_\ell}{\mathrm{d}E} \quad \text{and} \quad f_\ell(E) = \sum_{m=-\ell}^{\ell} f_{\ell m}. \tag{7}$$

In addition to Eq. (4), we also claim that

$$\left.\frac{\mathrm{d}S_{\ell m}}{\mathrm{d}x}\right|_{x=n} = \sigma_{n\ell m}, \tag{8}$$

$$\left.\frac{\mathrm{d}S_{\ell}}{\mathrm{d}x}\right|_{x=n} = \sigma_{n\ell}, \tag{9}$$

where $\sigma_{n\ell m}$ is the state-resolved excitation cross section and $\sigma_{n\ell}$ is the $n\ell$-resolved excitation cross section. The validity of Eqs. (4), (8), and (9) is demonstrated below.

We note that we did not make any assumptions about the projectile energy except it is sufficient to ionize the target. Therefore, those relationships are valid at all energies larger than the ionization potential of the atom. We also emphasize that we did not assume any particular functional form of the excitation cross sections and the corresponding singly differential ionization cross section when obtaining Eqs. (2), (5), and (7).

By construction, the piecewise functions $f_{\ell m}(E)$, $f_\ell(E)$, and $f(E)$ unify excitation and ionization. We now demonstrate that they can be used in studying a Coulomb three-body scattering problem, including the regions that were inaccessible in previous theories. We consider the benchmark system of $\bar{p} + \mathrm{H}(1s)$ collisions. It is a Coulomb three-body problem and has no analytic solution. It has been the subject of numerous experimental [6] and theoretical studies [7]. Above 1 keV incident energy, the protonium formation channel can be neglected, allowing one to describe $\bar{p} + \mathrm{H}$ scattering as a single-center problem. As a result, it serves as a useful test bed for developing new theoretical approaches and ideas. A number of different methods give reliable excitation cross sections for low-lying states as well as the total ionization cross section (TICS). We do not go into details as this is not the main subject of the present work. Instead, we refer the reader to a comprehensive review [7]. We only note that since publication of this review, a quantum-mechanical [8] and a semiclassical wave-packet [9] versions of the convergent close-coupling method were developed. These methods give not only integrated cross sections but also a fully differential picture of ionization. A missing piece of the puzzle was the absence of the information on excitation of the Rydberg states and threshold ionization. This paper provides the missing piece.

III. RESULTS AND DISCUSSION

The total wave function of the collision system satisfies Schrödinger's equation [10] with outgoing-wave boundary conditions. The method used for solving the scattering problem is based on expansion of the wave function using a set of suitably chosen basis states. Such a set should include the continuum. The continuum can be included, e.g., by diagonalizing the target Hamiltonian using an orthogonal Laguerre (Sturmian) basis [11] or using wave packets [9]. Here, we apply the convergent close-coupling approach to ion-atom collisions where the continuum is discretized using the nonorthogonal Sturmian basis [12] which we will refer to as the Coulomb-Sturmian (CS) one. The obtained CS pseudostates are used to expand the total scattering wave function for the $\bar{p} + \mathrm{H}$ system with some unknown expansion coefficients. Thereafter the method is similar to the wave-packet convergent close-coupling method detailed in Ref. [9]. Briefly, the expansion of the scattering wave function is substituted into the Schrödinger equation. This leads to a set of coupled equations for the expansion coefficients in the impact parameter representation. These equations are solved subject to the boundary condition reflecting the initial channel. Asymptotically, the expansion coefficients represent the transition probability amplitudes. Using the latter we can calculate $\sigma_{n\ell m}$, $\sigma_{n\ell}$, and σ_n for excitation of the negative-energy pseudostates.

The procedure for calculating the differential cross sections for ionization is given in Ref. [9]. In short, we begin from the general definition of the scattering amplitude in the *post* form [13,14]. If the collision leads to ionization, the final state of the system is described by the three-body Coulomb asymptotic state (CAS) representing three free particles. We bypass the need to use the CAS by inserting the identity operator constructed from the CS pseudostates into the *post* form of the scattering amplitude. This effectively reduces the CAS to a product of a plane wave for the relative motion of

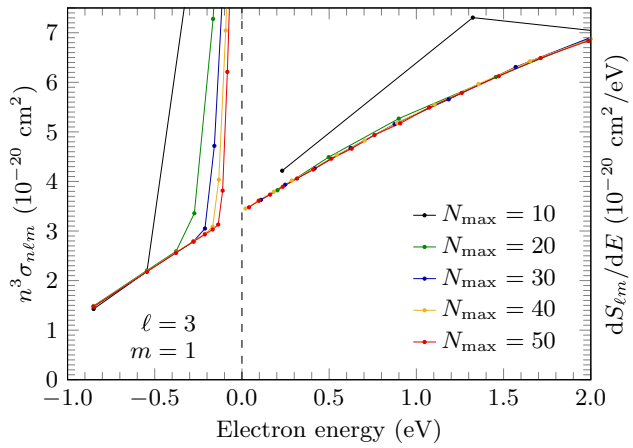

FIG. 1. The state-resolved excitation cross sections, multiplied by n^3, and the ℓm-partial SDCS for ionization as functions of electron energy for $\ell = 3$ and $m = 1$. The convergence of the results with respect to increasing $N_{\max}$ is shown.

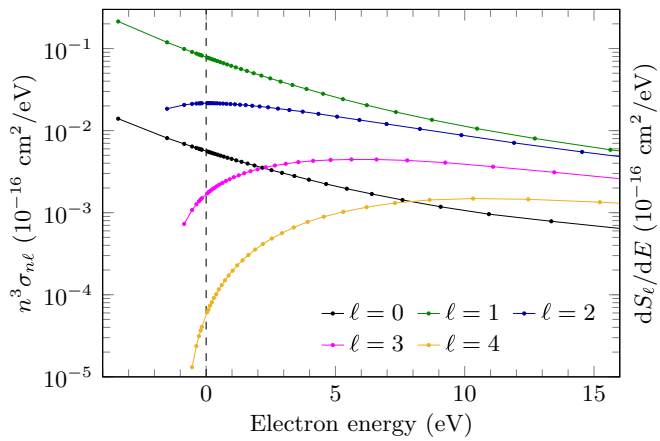

FIG. 2. The $n\ell$-resolved excitation cross sections, multiplied by n^3, and the ℓ-partial SDCS for ionization as functions of electron energy for $\ell = 0$–4.

the heavy particles and the Coulomb wave for the electron. As a result, the ionization amplitude is expressed in terms of the amplitudes for excitation of the positive-energy pseudostates and the projection of the pseudostates to the true continuum [9]. The $\mathrm{d}S_{\ell m}/\mathrm{d}E$ for ionization are obtained by integrating the fully differential cross sections. Alternatively, they can be expressed in terms of the cross sections for excitation of the positive-energy pseudostates. These two methods give identical results.

In coupled-channel calculations the accuracy of the results depends on the size of the basis. The basis is characterized by three parameters: the number of CS functions $N_{\max}$ for the s states, the maximum orbital quantum number $\ell_{\max}$, and the fall-off parameter λ. Then the number of the CS functions for each ℓ symmetry would be $N_{\max} - \ell$. As $N_{\max}$ and $\ell_{\max}$ increase, the results converge. By systematically increasing the size of the calculations, $\ell_{\max} = 5$ was found to be sufficient. When converged, the results do not depend on λ, however, the rate of convergence does. This has been tested using $\lambda = 0.4$, 0.5, and 0.6. The convergent results from these three sets of calculations were the same. By reducing λ we can reduce the energy of the highest pseudostate. This allows us to increase the density of the continuum discretization by increasing $N_{\max}$ without covering the part of the continuum that is not important. All the final results presented here are convergent to within a fraction of a percent. Hereafter, we refer to the basis size used in calculations as $(N_{\max}, \ell_{\max}, \lambda)$.

We have calculated the target excitation and singly differential ionization cross sections for $\bar{p} + \mathrm{H}(1s)$ collisions in a wide range of collision energies from 1 keV to 1 MeV. To avoid repetition, here we only present the results at 100 keV. However, the conclusions drawn from these results are also valid for all collision energies within the aforementioned range.

Figure 1 presents $n^3\sigma_{n\ell m}$ for excitation and $\mathrm{d}S_{\ell m}/\mathrm{d}E$ for ionization as functions of the electron energy for $\ell = 3$ and $m = 1$ obtained using bases $(N_{\max}, 5, 0.4)$ with increasing $N_{\max}$. The results are shown as dots connected by straight lines to guide the eye. We see a clear pattern of convergence with increasing $N_{\max}$. Furthermore, as $N_{\max}$ increases, $n^3\sigma_{n\ell m}$ approach $\mathrm{d}S_{\ell m}/\mathrm{d}E$ near the ionization threshold, confirming Eq. (5). However, it is notable that a few points on the negative-energy side deviate from the SDCS at the threshold for any value of $N_{\max}$. The reason for this can be explained by looking at the energy distribution of the pseudostates. For any basis size, the last few negative-energy pseudostates do not represent the eigenstates of the target. Instead, they mimic the remaining part of the discrete-energy spectrum. As mentioned above, Eq. (5) is valid for excitations of the eigenstates. If the energy of the pseudostate is different from the energy of the corresponding eigenstate (meaning the wave functions are different as well), the cross sections for excitation of such pseudostates do not obey Eq. (5). However, more and more negative-energy pseudostates accurately represent the eigenstates as $N_{\max}$ increases. In fact, a dominolike effect can be seen in Fig. 1, where an increasing number of $n^3\sigma_{n\ell m}$ fall into place and align with $\mathrm{d}S_{\ell m}/\mathrm{d}E$ along a smooth function of E as $N_{\max}$ increases. This confirms validity of Eqs. (5), (6), and (8). This convergence pattern is not just for the $\ell = 3, m = 1$ states. We have observed similar behavior for all ℓm values included in the calculations.

In Fig. 2, we plot $n^3\sigma_{n\ell}$ and $\mathrm{d}S_{\ell}/\mathrm{d}E$ for $\ell = 0$–4. The results that do not correspond to the eigenstates are not shown as they are not supposed to obey Eq. (7). In other words, we plot the piecewise function $f_\ell(E)$ at $x = n$. Having already demonstrated convergence with $N_{\max}$, here we only show the results obtained using basis (50,5,0.4). One can see that $n^3\sigma_{n\ell}$ and $\mathrm{d}S_{\ell}/\mathrm{d}E$ align and join at the ionization threshold for each value of ℓ confirming Eqs. (7) and (9). Furthermore, it is interesting to note different functional behaviors of $f_\ell(E)$ for different values of ℓ. For $\ell = 0$ and 1, $n^3\sigma_{n\ell}$ fall as they approach the ionization threshold. For the case of $\ell = 2$, $f_\ell(E)$ varies slowly across the ionization threshold. However, for $\ell > 2$ they increase towards the threshold. It is remarkable that Eq. (7) holds regardless.

In general, as seen in Fig. 2, the energies of the CS pseudostates are not aligned for different ℓ symmetry. However, from the data shown in Fig. 2, we can easily reconstruct $f_\ell(E)$ for each ℓ, e.g., using a polynomial fit. We can then sum up

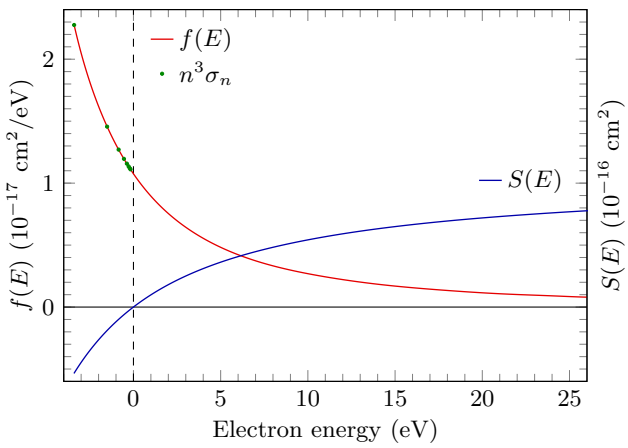

FIG. 3. $f(E)$ and $S(E)$ as functions of E. The dots represent σ_n multiplied by n^3. For $E \geqslant 0$, $f(E)$ represents the SDCS.

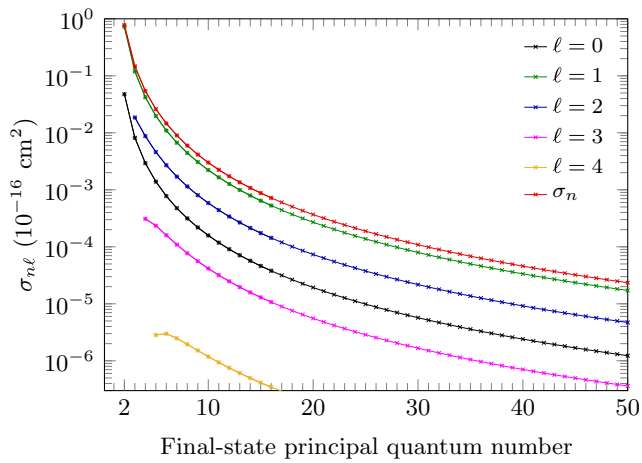

FIG. 4. The $n\ell$- and n-resolved excitation cross sections as functions of the final-state principal quantum number n for $\ell = 0$–4. The crosses represent $\sigma_{n\ell}$ and σ_n obtained using f_ℓ and f resulting from the (50,5,0.4) basis calculation. The pluses represent the corresponding results obtained directly from the (130,5,0.4) basis calculation.

all $f_\ell(E)$ to get $f(E)$ as a continuous function. By integrating $f(E)$ over E we also recover $S(E)$. Functions $f(E)$ and $S(E)$ are plotted in Fig. 3. We see that beginning from negative energies, $f(E)$ falls as it approaches the threshold. This shows that generally the transition across the threshold is not always a slowly varying function of energy as suggested by Rudd and Macek [5]. The figure also shows $n^3\sigma_n$ which coincides with $f(E_n)$ as expected. It is extraordinary that the piecewise functions work for excitation of any state. When the target is initially in the 1s state, considered here, the formula works starting literally from $n = 2$.

Having demonstrated the validity of Eqs. (2)–(9), next we use them to obtain the state-resolved excitation cross sections for any bound state including the Rydberg ones with arbitrarily high energies. Furthermore, they also allow us to obtain the SDCS for ionization at, and arbitrarily close to, the threshold. To this end, we simply use piecewise functions $f_{\ell m}(E)$, $f_\ell(E)$, and $f(E)$. To demonstrate the reliability of this approach, we perform two different calculations. The first calculation employs basis (50,5,0.4), and is used to reconstruct $f_{\ell m}(E)$, $f_\ell(E)$, and $f(E)$. The second calculation uses a very large basis of (130,5,0.4). This increases the number of the eigenstates reproduced accurately. As a result we obtain accurate converged excitation cross sections up to a reasonably high principal quantum number that can be tested against the corresponding results obtained using $f_{\ell m}(E)$, $f_\ell(E)$, and $f(E)$. We find that $\sigma_{n\ell m}$, $\sigma_{n\ell}$, and σ_n for high-lying states not explicitly included in the (50,5,0.4) basis calculation, but obtained using $f_{\ell m}(E)$, $f_\ell(E)$, and $f(E)$, reproduce the corresponding converged results obtained directly using the (130,5,0.4) basis in all cases. This shows that even without explicitly including the high-lying states in the basis, the calculations can give the cross sections for these states due to the regular and smooth nature of $f_{\ell m}(E)$, $f_\ell(E)$, and $f(E)$.

The crosses in Fig. 4 represent $\sigma_{n\ell}$ and σ_n up to $n = 50$ obtained using f_ℓ and f resulting from the (50,5,0.4) basis calculation. The pluses represent the corresponding results obtained directly using the (130,5,0.4) basis. The agreement is perfect (the results are almost identical with the crosses overlapping with the pluses). Note that out of the pseudostates included in the (50,5,0.4) basis calculation only a small portion has negative energies. For instance, out of the 50 s states only 14 have negative energies and only 9 correspond to the eigenstates. It is extraordinary that the calculation with a relatively small basis is capable of giving the complete set of excitation cross sections due to the power of Eqs. (2)–(9). We can also see that for $n \geqslant 2$, p-state cross sections are dominant. As ℓ increases further, each next set of $n\ell$-resolved cross sections falls by an order of magnitude. This shows that only the first few values of ℓ significantly contribute to σ_n even for the Rydberg states with n as high as 50. Though the results are shown for $2 \leqslant n \leqslant 50$, the method is expected to work for arbitrarily high n as the limits of $f(E)$ and $f_\ell(E)$ as $n \to \infty$ exist and are finite due to Eqs. (2) and (7).

Using Eq. (5) and the piecewise function $f_{\ell m}(E)$ we can calculate the state-selective cross sections for arbitrary states. As an example, in Fig. 5 we show $\sigma_{n\ell m}$ up to $n = 100$ for

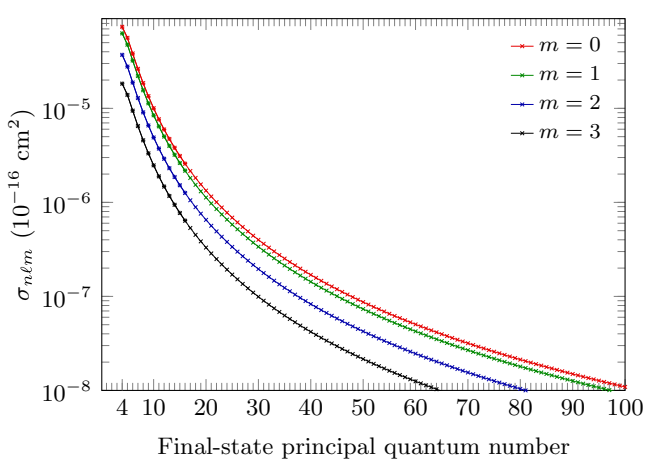

FIG. 5. The $n\ell m$-resolved excitation cross sections as functions of the final-state principal quantum number n for $\ell = 3$ and $m = 0$–3. The crosses represent $\sigma_{n\ell m}$ obtained using $f_{\ell m}$ resulting from the (50,5,0.4) basis calculation. The pluses represent the corresponding results obtained directly using the (130,5,0.4) basis.

$\ell = 3$ and all values of m. Again, the crosses represent $\sigma_{n\ell m}$ obtained using $f_{\ell m}$ resulting from the (50,5,0.4) basis calculation. The pluses represent the corresponding results obtained directly from the (130,5,0.4) basis calculation.

Finally, the method gives the total excitation cross section, $\sum_{n=2}^{\infty} \sigma_n$. At 100 keV incident energy, it converges to four significant digits when the first 50 shell cross sections are summed up giving 1.051×10^{-16} cm^2. One can also calculate the SDCS at the ionization threshold. It is given by $f(0)$. The SDCS at the threshold is found to be 1.075×10^{-17} cm^2/eV. Obviously, $S(E_{\text{total}})$, representing the integral of $f(E)$ from 0 to E_{total}, gives the TICS. We find TICS $= 1.004\times10^{-16}$ cm^2, which is accurate to four significant digits and in excellent agreement with experiment [6]. Other physical properties of function $S(E)$ remain to be investigated.

IV. CONCLUSION

We proposed a unified treatment of atomic excitation and ionization. We demonstrated that the state-resolved excitation cross sections multiplied by n^3 and the corresponding partial singly differential ionization cross section form two parts of a single continuous function. This allowed us to obtain the excitation cross section for any state including high-lying Rydberg states and the energy-differential ionization cross section at, and arbitrarily close to, the threshold.

Furthermore, the proposed method can be used in experimental and theoretical studies of other atomic collisions involving arbitrary projectiles. For example, accurate measurements or calculations of the first few excitation cross sections and some small part of the SDCS of ionization in an arbitrary collision system can be used as input to construct the corresponding $f(E)$. This function will contain information on all the missing parts of the excitation cross sections and the SDCS. The accuracy of the outcome only depends on the accuracy of the input data. The method may also lead to further investigations of the threshold phenomena [15] including threshold ionization in $(e, 2e)$ [16] and various atomic collisions [17] as it allows to approach the threshold as closely as necessary and actually reach it, which was impossible so far. The laser excitation of positronium into Rydberg states [18] and further ionization [19] is another avenue that can be explored using the new method.

ACKNOWLEDGMENTS

This work was supported by the Australian Research Council. We acknowledge the resources and services of the Pawsey Supercomputing Centre and the National Computing Infrastructure. N.W.A. acknowledges support through the Australian Government Research Training Program.

[1] A. Sommerfeld, *Atombau und Spektrallinien* (F. Vieweg & Sohn, Braunschweig, 1924), Vol. 1.

[2] J. Berkowitz, *Photoabsorption, Photoionization, and Photoelectron Spectroscopy* (Academic Press, New York, 1979).

[3] H. A. Bete and R. Jackiw, *Intermediate Quantum Mechanics*, 3rd ed. (CRC Press, Boca Raton, FL, 1997).

[4] J. R. Oppenheimer, On the quantum theory of the capture of electrons, Phys. Rev. **31**, 349 (1928).

[5] M. E. Rudd and J .H. Macek, Mechanisms of electron production in ion–atom collisions, in *Case Studies in Atomic Physics*, edited by E. W. McDaniel and M. R. C. McDowell (Elsevier, Amsterdam, 1974), Chap. 2, pp. 47–136.

[6] H. Knudsen, U. Mikkelsen, K. Paludan, K. Kirsebom, S. P. Møller, E. Uggerhøj, J. Slevin, M. Charlton, and E. Morenzoni, Ionization of atomic hydrogen by 30 1000 keV antiprotons, Phys. Rev. Lett. **74**, 4627 (1995).

[7] T. Kirchner and H. Knudsen, Current status of antiproton impact ionization of atoms and molecules: Theoretical and experimental perspectives, J. Phys. B: At. Mol. Opt. Phys. **44**, 122001 (2011).

[8] I. B. Abdurakhmanov, A. S. Kadyrov, I. Bray, and A. T. Stelbovics, Differential ionization in antiproton–hydrogen collisions within the convergent-close-coupling approach, J. Phys. B: At. Mol. Opt. Phys. **44**, 165203 (2011).

[9] I. B. Abdurakhmanov, A. S. Kadyrov, and I. Bray, Wave-packet continuum-discretization approach to ion-atom collisions: Nonrearrangement scattering, Phys. Rev. A **94**, 022703 (2016).

[10] E. Schrödinger, Quantisierung als eigenwertproblem, Ann. Phys. **384**, 361 (1926).

[11] I. B. Abdurakhmanov, A. S. Kadyrov, I. Bray, and A. T. Stelbovics, Coupled-channel integral-equation approach to antiproton–hydrogen collisions, J. Phys. B: At. Mol. Opt. Phys. **44**, 075204 (2011).

[12] M. Rotenberg, Theory and applications of Sturmian functions, Adv. At. Mol. Phys. **6**, 233 (1970).

[13] A. S. Kadyrov, I. Bray, A. M. Mukhamedzhanov, and A. T. Stelbovics, Coulomb breakup problem, Phys. Rev. Lett. **101**, 230405 (2008).

[14] A. S. Kadyrov, I. Bray, A. M. Mukhamedzhanov, and A. T. Stelbovics, Surface-integral formulation of scattering theory, Ann. Phys. **324**, 1516 (2009).

[15] E. P. Wigner, On the behavior of cross sections near thresholds, Phys. Rev. **73**, 1002 (1948).

[16] G. H. Wannier, The threshold law for single ionization of atoms or ions by electrons, Phys. Rev. **90**, 817 (1953).

[17] H. Klar, Threshold ionization of atoms by positrons, J. Phys. B: At. Mol. Opt. Phys. **14**, 4165 (1981).

[18] D. B. Cassidy, T. H. Hisakado, H. W. K. Tom, and A. P. Mills, Jr., Efficient production of Rydberg positronium, Phys. Rev. Lett. **108**, 043401 (2012).

[19] A. M. Alonso, L. Gurung, B. A. D. Sukra, S. D. Hogan, and D. B. Cassidy, State-selective electric-field ionization of Rydberg positronium, Phys. Rev. A **98**, 053417 (2018).